Article

Active Biochemical Regulation of Cell Volume and a Simple Model of Cell Tension Response

Jiaxiang Tao[1] and Sean X. Sun[1,*]
[1]Department of Mechanical Engineering, Department of Biomedical Engineering, and Johns Hopkins Physical Sciences-Oncology Center, Johns Hopkins University, Baltimore, Maryland

ABSTRACT Active contractile forces exerted by eukaryotic cells play significant roles during embryonic development, tissue formation, and cell motility. At the molecular level, small GTPases in signaling pathways can regulate active cell contraction. Here, starting with mechanical force balance at the cell cortex, and the recent discovery that tension-sensitive membrane channels can catalyze the conversion of the inactive form of Rho to the active form, we show mathematically that this active regulation of cellular contractility together with osmotic regulation can robustly control the cell size and membrane tension against external mechanical or osmotic shocks. We find that the magnitude of active contraction depends on the rate of mechanical pulling, but the cell tension can recover. The model also predicts that the cell exerts stronger contractile forces against a stiffer external environment, and therefore exhibits features of mechanosensation. These results suggest that a simple system for maintaining homeostatic values of cell volume and membrane tension could explain cell tension response and mechanosensation in different environments.

INTRODUCTION

Eukaryotic cells can actively exert mechanical forces on their extracellular environment. These forces have been measured in two- (2D) and three-dimensional (3D) cell cultures (1-4), and have been shown to be important not only during cell migration, tissue and organ formation, and development, but also during cell-volume control in response to osmotic changes (5). Many experiments have shown that cells on stiffer substrates apply stronger contractile forces (1,6,7). Biochemical signaling pathways have been implicated in this active force generation. Notably, GTPases such as the Rho family of proteins, are part of the signaling pathway that controls myosin II assembly and force generation. The active form of Rho phosphorylates ROCK, which then activates the myosin light chain (MLC) (8-12). This leads to the assembly of myosin minifilaments and an increase in contractile forces. Remarkably, Rho itself also responds to externally applied mechanical forces. When cells are mechanically pulled by attached magnetic beads, the active form of Rho also increases and then diminishes in time, presumably correlated with changes in contractile force (12). Related phenomena are seen when cells are subjected to pipet suction. Here, an increase in myosin accumulation is observed at the location of suction force (13,14), although Rho activation was not directly measured in those experiments. Finally, when cells are subjected to osmotic shock, which changes the mechanical tension across the cell-membrane cortex, myosin contraction has been implicated in restoring the cell volume to preshock values (5,15). More recent studies have shown that mechanosensitive (MS) membrane channels can regulate the activity of Rho and catalyze the conversion from the inactive form to the active form (8,16-19). These experiments are beginning to reveal the feedback loop between active cell force generation and mechanical tension.

In this article, we mathematically examine such a feedback mechanism that controls cell active contraction using a simple mechanical model coupled to a biochemical network. To keep the cell geometry simple and remove complexities from cell adhesions, we consider suspended or mitotic cells where they are spherical, and cylindrical cells between flat cantilevers with fixed adhesion area. The latter situation has been elegantly examined recently in experiments (20,21). We first describe the balance of forces at the cell boundary, which is made of cell membrane and an actomyosin cortex. By modeling the cortex as an active gel with rapid actin turnover (22-24), we find that the hydrostatic pressure difference across the cell membrane is balanced by active cortical contraction, passive stress from cortical flow, and membrane tension. Indeed, cell osmotic pressure is partially controlled by MS ion channels and ion transporters in the membrane (15,25). Recent studies have shown that the MS channel TRPIV is involved in activating Rho in response to osmotic pressure changes (16,17). Related experiments in *Drosophila* cells indicate that the transmembrane protein Toll can activate Rho and contraction (8,18,19). Further evidence also suggests that membrane tension is a global signal that controls cell polarization (26). Labeling of the active form of Rho in

Submitted January 26, 2015, and accepted for publication August 19, 2015.
*Correspondence: ssun@jhu.edu
Editor: Charles Wolgemuth.

0006-3495/15/10/1541/10
http://dx.doi.org/10.1016/j.bpj.2015.08.025

live cells showed that Rho is preferentially activated near the cell leading edge, where membrane tension is likely high (27,28). Here we demonstrate how to model this system mathematically, and compute the cell response to external changes in osmolarity as well as externally applied forces.

The model appears to unify a number of related phenomena in cell mechanics. First, the proposed system is able to maintain a relatively constant cell volume in response to osmotic changes. Osmotic shocks lead to changes in the hydrostatic pressure difference and membrane tension and cause water flow across the cell membrane. In our model, this leads to ion flows across the membrane and changes in active contraction. The result is a robust adjustment of cell volume and membrane tension back to the preshock values, in accordance with single-cell experiments (5). We also show that neither ion flow nor active contraction alone leads to robust adaptation to osmotic shocks. Both systems are needed to obtain robust volume control. Second, when a cell is stretched between two cantilevers, external mechanical pulling also leads to water flow and membrane-tension changes. This increases active contractile forces that again try to restore cell volume and membrane tension. Cell active contraction therefore changes over time. The contraction dynamics of the cell depends on the rate of pulling, and the final cell tension depends on the total amount of deformation. Third, when a cell is subjected to a jump in externally applied mechanical force, Rho becomes activated and there is a membrane tension jump. However, Rho activation recedes over time because of ion flows, and the membrane tension is restored to prejump values, in accordance with dynamics observed by Zhao et al. (12). Fourth, our model is able to predict that the cell will exert larger steady contractile force against a stiffer substrate. The steady-state cell volume also varies depending on cantilever stiffness. This result indicates that our model can explain some features of cell mechanosensation where stiffness of the cell substrate influences cell contractility. It also indicates that active control of cell contraction can explain cell volume dynamics as well as cellular response to externally applied forces.

We begin by considering mechanics of the cell cortex and membrane subjected to excess osmotic pressure in the cell. We then describe the regulation of osmotic pressure by membrane channels and ion pumps, and a simple model of Rho regulation of myosin contraction. Model predictions for cells subjected to osmotic shocks or mechanical shocks, such as a sudden application of pulling force, are analyzed. Detailed predictions of cell responses to mechanical forces and the mechanism of strain-rate-dependent force response are discussed. We also demonstrate that the model predicts increasing levels of myosin activation when the cell contracts against substrates of increasing stiffness. In comparison with our previous work on cell volume control (25), which considered an elastic constitutive relation for the cell cortex, this work focuses on dynamics for a liquid-like cortex and active control of myosin contraction. The liquid-like cortex is likely the correct description for most tissue cells under normal circumstances. Therefore, our model suggests that the cell volume exists as a stable steady state of a dynamically controlled biochemical system.

MATERIALS AND METHODS

Force balance at the cell surface

A typical cell is bounded by a surface consisting of an outer plasma membrane and an actomyosin cortex. The plasma membrane is adhered to the actomyosin cortical layer through transmembrane proteins (Fig. 1). The membrane is typically 5 nm in thickness, but the cortical layer thickness, h, is 200–500 nm (29). Within the cell cortex, actin filaments rapidly turn over and small myosin motor assemblies exert active contractile forces (23,30). There are also dynamic actin cross-linking proteins that can potentially alter the mechanics of the cortex (30). Although the molecular details of the cortex are complex, it can be generically modeled as an active viscoelastic gel-like fluid. Being a viscoelastic fluid, it does not have a reference geometry and will flow under mechanical perturbations. Therefore, force balance and cortex geometry alone cannot determine the global cell shape and volume. To simplify matters in this article, we will ignore actin dynamics associated with focal adhesions and focus on cells with fixed or no contact with substrates.

The cytoplasm is crowded with proteins, RNA, and ions; the osmotic pressure inside the cell is therefore generally higher than that of the extracellular milieu. Therefore, there is an osmotic pressure difference, $\Delta\Pi = \Pi_{in} - \Pi_{out}$, between the inside and outside of the cell. Π_{in} is related to the total osmolytes, n, in the cell, or $\Pi_{in} \sim RTc_{in} \propto n/V$, where V is the cell volume (Fig. 2 *A*), R is the gas constant, and c_{in} is the osmolyte

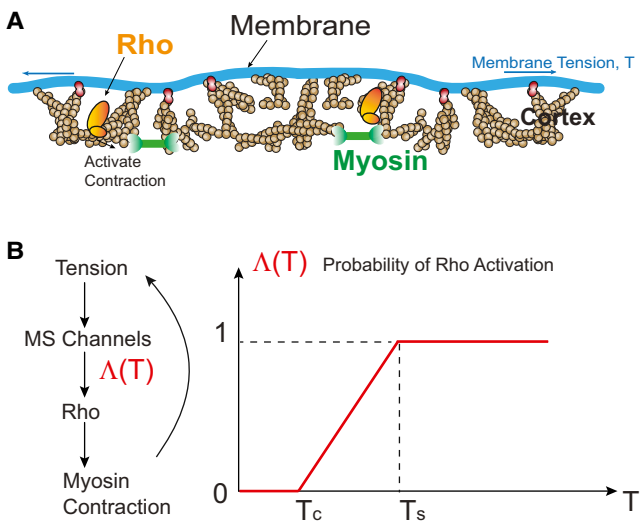

FIGURE 1 (*A*) Illustration of the Rho signaling pathway that activates myosin assembly and active contraction in the cell cortex. At mechanical equilibrium, the membrane tension must balance both osmotic pressure in the cell and active contraction in the cortex (Eq. 1). (*B*) In our model, we consider membrane-tension changes that activate MS channels, which then activate Rho and myosin contraction. The contractile force negatively feeds back to membrane tension. The probability of Rho activation, $\Lambda(T)$, starts to increase at a critical tension, T_c, and saturates at T_s. To see this figure in color, go online.

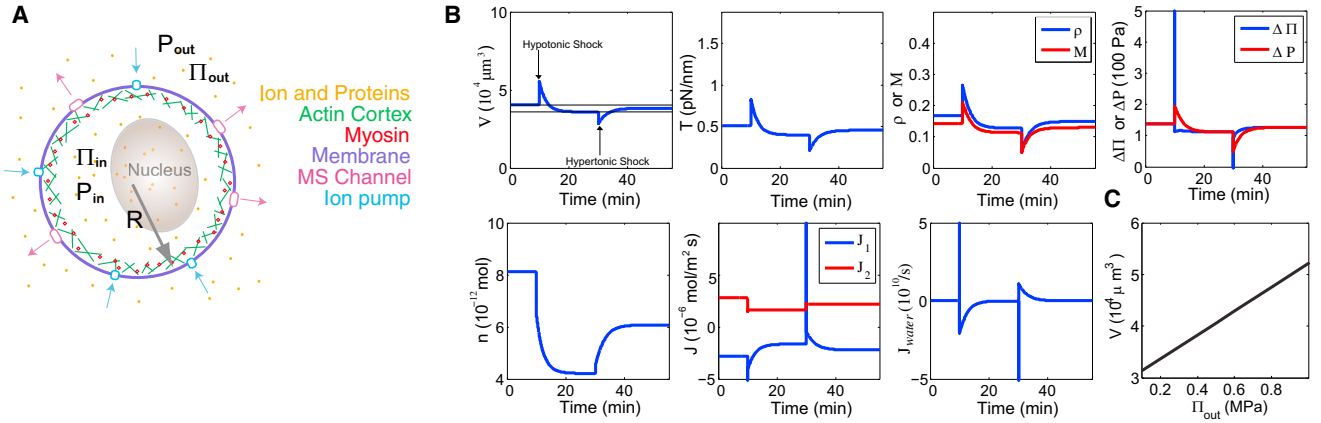

FIGURE 2 Model calculations for a spherical cell during osmotic shock. (*A*) Cartoon of the cell showing components important in our model. For the active ion pumps, we have used $\Delta\Pi_c = 1.1\Pi_{out}$. (*B*) The cell is subjected to a hypotonic shock and then a hypertonic shock. The shock magnitudes are 0.5 Π_{out} and then 0.75 Π_{out}. The cell volume can recover to close to the preshock value. Indeed, volume, membrane tension, Rho-MLC activation level, and pressure difference all can recover, meaning that the cell can adapt to the new osmotic environment. There is a slight overshoot after recovery, because $\Delta\Pi_c$ is proportional to Π_{out}. (*C*) The steady-state cell volume depends on Π_{out}. The model predicts that the steady volume after recovery is smaller after a hypotonic shock. Here, $\Delta\Pi_c = 1.1\Pi_{out}$. To see this figure in color, go online.

concentration inside. Water will flow in response to this osmotic pressure difference, but at static equilibrium, the osmotic pressure difference equals the hydrostatic pressure difference: $\Delta\Pi = \Delta P$. The hydrostatic pressure difference is balanced by tension in the membrane and mechanical stress in the cortex. Using a simple active gel model, force balance can be solved for a cell surface element (see the Supporting Material for details). It can be shown that the passive viscous shear stress in the cortex is small at steady state, and the active stress is the dominant contribution. The resulting force balance is simple for a spherical cell with radius R:

$$\frac{\Delta PR}{2} = T + \sigma^a h, \tag{1}$$

where σ^a is the nonzero diagonal part of the active stress tensor: $\sigma_{active} = -\sigma^a(\mathbf{e}_\phi \otimes \mathbf{e}_\phi + \mathbf{e_0} \otimes \mathbf{e_0})$, and T is the tension in the membrane. Here, we assume that myosin contracts in directions tangential to the cell surface. In general, for an arbitrary cell shape with local mean curvature C, where $C = \nabla \cdot \mathbf{n}$, the hydrostatic pressure is balanced by

$$\frac{\Delta P}{2C} = T + \sigma^a h, \tag{2}$$

and $\mathbf{n}$ is the local cell surface normal vector. Given that actin polymerization and turnover is relatively fast, the above force-balance condition is reached within tens of seconds. In deriving the force balance condition, we have assumed that the cortical mass and density are constant, and the cortex behaves as a Newtonian fluid. Actomyosin networks, however, have complex mechanical properties, and the physics of cortical flow has been extensively discussed (23,31). The simple approximations followed here allowed us to obtain the analytical estimates above.

Biochemical regulation of myosin contraction

The force-balance relation in Eq. 1 alone does not determine global cell shape and size. This is achieved by dynamic myosin contraction, i.e., σ^a is not a constant, but changes in response to mechanical forces applied to the cell. From the force-balance relation in Eq. 1, we see that osmotic pressure, hydrostatic pressure, or any mechanical forces on the cell will change both membrane tension and tension in the cortex. Therefore, we propose that membrane tension could be the upstream signal that catalyzes the activation of Rho. Other possibilities also exist, e.g., transient cortical stress could change myosin binding to actin and power-stroke kinetics (13,32). This additional complexity is discussed later in the Discussion and Supporting Material. All these models suggest a feedback mechanism where increases in membrane tension and mechanical stress in the cortex lead to increasing myosin contraction and σ^a. This then restores the membrane tension and passive mechanical stress. Indeed, our model predicts that the cell can maintain essentially a constant membrane tension with this mechanism.

The chemical signaling network we propose to examine is shown in Fig. 1. Rho activation is triggered by membrane tension, T. Rho activates the MLC, which increases the fraction of myosin minifilaments, M. The concentration of myosin minifilaments is directly proportional to the active stress,

$$\sigma^a = K_{max} M, \tag{3}$$

where K_{max} is a maximum contractile stress parameter and M is the fraction of activated myosin. K_{max} is the maximum stress the cell can exert if all of the myosins are activated. The biochemical equations are

$$\begin{aligned} \frac{\partial \rho}{\partial t} &= a_1 \Lambda(T)(1-\rho) - d_1 \rho \\ \frac{\partial M}{\partial t} &= a_2(1-M)\rho - d_2 M, \end{aligned} \tag{4}$$

where a_1 and d_1 are the activation and deactivation rates, respectively, of Rho; ρ and M are percentages of activated Rho and myosin, respectively; and a_2 and d_2 are the myosin assembly and disassembly rates, respectively. Here, for simplicity, we do not explicitly include ROCK in the pathway. Instead, ROCK dynamics is included in the equation for Rho by using effective rate constants a_1 and d_1. Λ is an activation function of ρ, which depends nonlinearly on membrane tension, T. We propose that $\Lambda = (T - T_c/T_s - T_c)$ when $T_c < T < T_s$. $\Lambda = 1$ when $T > T_s$ and $\Lambda = 0$ when $T < T_c$. T_c is the critical membrane tension at which Rho activation starts and T_s is a saturating tension (Fig. 1). The functional form of Λ is essentially the same as a Michaelis-Menten type of enzymatic kinetics.

We also note that within our model, it is possible to consider nonlinear behavior in the mechanics of the actin cortex and strain-hardening behavior in actin networks. Multiple experiments show that there is a change in the number of actin cross-linkers when cells are subjected to rapid changes in

force (13,20). This complex behavior would influence myosin assembly and contraction. These results suggest that myosin assembly and disassembly rates, a_2 and d_2, depend on transient passive stress in the cortex. One possible way to incorporate this effect is to write

$$a_2 = a_{20}(1 + f(T_{\text{shear}})), \tag{5}$$

where a_{20} is a constant and T_{shear} is a passive transient force per unit length in the cortex (see the Supporting Material for details). $f(T_{\text{shear}})$ is an activation function that depends on T_{shear}. For Newtonian fluids, T_{shear} is proportional to the flow rate in the cortex. This phenomenological model is consistent with the idea that myosin assembly and force production depend on the shear stress (rate of deformation) in the cortex. This model is also related to the observed strain-rate-dependent force change (see Fig. 4). However, the details of the model will have to depend on a better understanding of the relationship between cortex mechanics and myosin assembly and contraction. Other mechanisms that regulate myosin contraction are also possible; for example, calcium influx from tension change can also regulate myosin contraction (33,34). It is likely that multiple mechanisms are at play to different degrees in different kinds of cells.

Active regulation of cell volume and membrane tension

In addition to active regulation of myosin contraction, the cell can also adjust its internal osmotic pressure, Π_{in}, leading to cell-volume adaptation to osmotic shocks (5,15). Equations for water and ion fluxes were discussed in a recent article (25). They are

$$\begin{aligned} \frac{\partial V}{\partial t} &= -\alpha A(\Delta P - \Delta\Pi) \\ \frac{\partial n}{\partial t} &= A(J_1 + J_2), \end{aligned} \tag{6}$$

in which V and A are cell volume and surface area, respectively. ΔP and $\Delta\Pi$ are hydrostatic and osmotic pressure differences across the membrane. $\partial V/\partial t$ is the rate of cell-volume change due to water flow. n is the total number of osmolytes in the cell. J_1 is the ion flux out of the cell through passive membrane channels. These passive ion channels could be MS and open in response to changes in membrane tension. Thus, $J_1 = -\beta\Lambda'(T)\Delta\Pi$. The negative sign indicates the outflow of ions. $\Lambda'(T)$ is a function similar to $\Lambda(T)$ in Fig. 1 *B*, and it depends on parameters T_1 and T_2, which are the critical and saturation tensions of MS channels.

J_2 describes flux through active ion pumps, which pump against concentration gradients. J_2 can be computed from a simple channel model. Assuming that the pump uses energy input, ΔG_{a}, to generate a pump force of $\Delta G_{\text{a}}/\delta$, where δ is the membrane thickness, the steady-state flux through a single channel is approximately $j_2 = -D\partial c/\partial x - D/k_{\text{B}}T(\Delta G_{\text{a}}/\delta)c$, where c is the ion concentration profile within the channel and D is an effective diffusion constant. c satisfies boundary conditions $c(0) = c_{\text{in}}$ and $c(\delta) = c_{\text{out}}$. This gives the single pump flux as

$$j_2 = \frac{D\Delta G_{\text{a}}}{k_{\text{B}}T\delta}\left(\frac{\Delta\Pi e^{-\Delta G_{\text{a}}/k_{\text{B}}T}}{RT(1 - e^{-\Delta G_{\text{a}}/k_{\text{B}}T})} - c_{\text{out}}\right). \tag{7}$$

From this, we can obtain $\Delta\Pi_{\text{c}}$, the critical concentration at which the flux is zero:

$$\Delta\Pi_{\text{c}} = \Pi_{\text{out}}\left(e^{\Delta G_{\text{a}}/k_{\text{B}}T} - 1\right). \tag{8}$$

The total pump flux therefore can be written as

$$J_2 = n_{\text{a}} j_2 = -\gamma(\Delta\Pi - \Delta\Pi_{\text{c}}), \tag{9}$$

where γ is another effective permeation constant that contains the number density of the ion pumps, n_{a}. In general, depending on the molecular mechanism of the ion pump, the flux expression, J_2, can be quite complicated. If multiple species of ions are considered, the different flux would depend on individual ion concentrations. Equation 17 is the simplest model. More complex models, such as those in Gao et al. (35) and Armstrong (36), can be explored as well.

Equations 1, 3, 4, and 6 are six equations that describe cell-volume changes in response to changes in osmotic pressure, mechanical forces, and active motor activity. For a spherical cell, the unknowns are $(\rho, M, T, \Delta P, \sigma^{\text{a}}, R,$ and $n)$. These equations are not closed, and they require one other relationship, the constitutive law for the cell membrane, which relates the membrane tension to overall area changes of the membrane. A simple linear relationship (37) is

$$T = \kappa\left(\frac{A - A_0}{A_0}\right), \tag{10}$$

where κ is an effective elastic modulus and A_0 is the reference membrane area when it is not under tension. A_0 is set by the total number of lipid molecules. A_0 also can depend on lipid trafficking, which may be also triggered by membrane tension (38,39). In addition, A_0 includes possible entropic properties of the membrane and reflects the fact that the membrane is typically highly folded in the cell (40). A is the stretched membrane area. Here, κ could arise from entropic elasticity. Lipid trafficking occurs on a timescale of hours, and here we regard A_0 as a constant.

RESULTS

Robust control of cell volume and membrane tension

Using this model, we can mathematically describe the dynamics of the cell volume during osmotic shock (Fig. 2). Results show the behavior of a stable dynamical system arising from active control, where a stable volume is determined not by any reference geometry but by cell parameters such as K_{max} and n. A sudden decrease in Π_{out} causes water influx into the cell across the membrane, decreasing ΔP, which leads to an increase in membrane tension. Membrane tension changes trigger chemical activation of the Rho-MLC pathway, as well as opening of ion channels at the cell surface. This active contraction and the ion fluxes help membrane tension to recover from the initial changes. Because the cell cortex is a viscoelastic fluid without any reference shape, active contractile stress must adjust to maintain a constant cell volume. If there is no active control, the cell volume cannot adapt properly to osmotic shocks (Fig. 3 *A*). Under hypertonic shock, ion pumps are essential in regulating cell volume, since myosin contraction does not play a role. Without ion fluxes, the cell is unable to recover after hypertonic shock (Fig. 3). Without myosin active contraction, the cell is still able to recover, but there is a large overshoot in the cell-volume change after recovery.

Critical parameters in this volume adaptation system are $\Delta\Pi_{\text{c}}$, permeation constants γ and β, and maximum contractile stress, K_{max}. These parameters all can influence the final steady-state volume of the cell (Figs. 3 *B* and S2). As we noted in Eq. 8, $\Delta\Pi_{\text{c}}$ is a function of Π_{out}; therefore, the

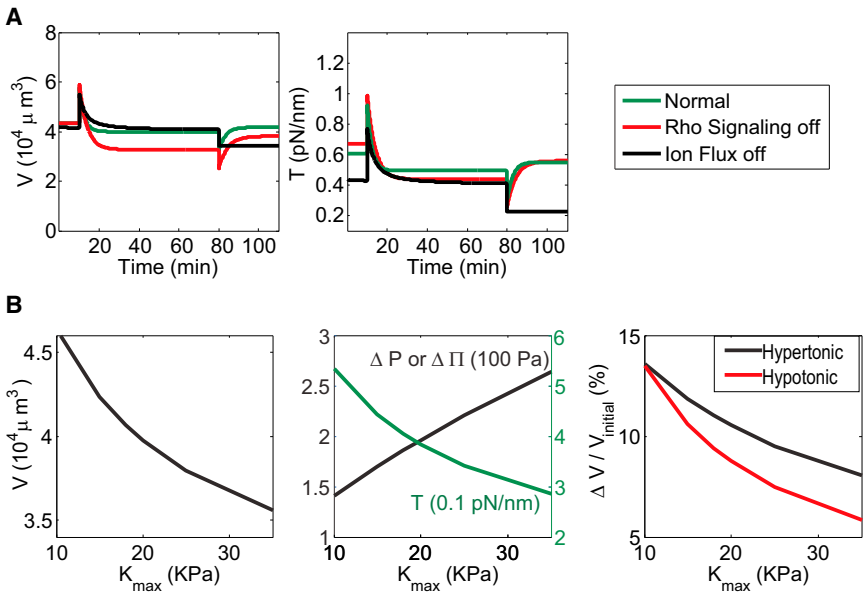

FIGURE 3 Biochemical control of contraction and ion permeation help to maintain cell volume and membrane tension. (*A*) The model predicts that when Rho signaling control of myosin is turned off and σ^a is a constant (*red line*), or ion fluxes are turned off and $J_1 = J_2 = 0$ (*black line*), the cell does not recover cell volume or membrane tension effectively. When both systems are active (*green line*), the cell volume and membrane tension can effectively maintain a homeostatic value. Note that the initial cell volume before shock is kept the same in the model, but different initial starting points for n and σ^a are needed to achieve the same initial volume. (*B*) Steady-state cell volume, membrane tension, and hydrostatic pressure are determined by maximum possible myosin active stress (K_{max}) and Π_{out}. As K_{max} increases, the cell volume decreases and pressure increases. The membrane tension decreases. Decreasing Π_{out} decreases steady-state cell volume, although the volume does transiently increase at first. The degree of volume overshoot, $\Delta V/V_{initial}$, after osmotic shock also depends on K_{max}. To see this figure in color, go online.

cell volume after recovery is not the same as before the osmotic shock (Fig. 2 *C*). Instead, assuming everything else is constant within the cell, the steady-state cell volume decreases as Π_{out} decreases, even though volume initially increases transiently after Π_{out} decreases. γ and β are permeation constants of the passive and active ion channels. These parameters are related to overall expression levels of these membrane proteins and their molecular properties. We see that these parameters determine the overall steady-state solute content in the cell, and therefore the steady-state volume (Fig. S2).

K_{max} is a parameter that describes the maximum active contractile stress the cell can generate when all available myosin is fully activated. Myosin active stress also depends on an intact cell cortex, so depolymerizing actin would impact K_{max}. We see that the steady-state cell volume and membrane tension decline as K_{max} increases, suggesting that the cell volume will increase if active stress is reduced (Fig. 3). Larger K_{max} also increases the hydrostatic pressure difference at steady state. However, larger K_{max} provides stronger control of cell volume after osmotic shocks (Fig. 3 *B*), where the volume change after osmotic shock is minimized with respect to before the shock.

The rate of cell-volume adaptation depends on the water permeation parameter, α, and the chemical rate constants a_1, a_2, d_1, and d_2 that govern the speed of Rho and myosin activation. In this work, we have set these rate constants such that adaptation occurs within 10 min. This is consistent with results seen in Stewart et al. (5) and Zhao et al. (12), where activation of Rho occurred $\sim$ 5 min after cells were pulled by magnetic beads. This is also the same timescale as for myosin activation after pipet aspiration, which changes the hydrostatic pressure difference across the membrane (13).

As mentioned earlier, we have assumed that the lipid reference area, A_0, is a constant and that cell volume changes from fluxes through membrane channels such as aquaporins. Cells can also change volume through endocytosis, whose rates should also depend on membrane tension. At longer timescales of hours, lipid trafficking from the Golgi to the cell surface can occur. This would potentially change A_0, and it suggests a third mechanism of cell membrane-tension control. Previous work suggests that membrane tension can be controlled if the rates of lipid addition and subtraction are functions of membrane tension (41). This phenomenon is likely if the membrane tension has changed persistently for long periods, and myosin contraction and ion transport are unable to restore membrane tension. Lipid trafficking can provide the final mechanism of restoring cell integrity.

A simple model of cell tension homeostasis

The proposed model not only can describe how cells respond to osmotic changes, but can also predict cell response to external applied mechanical forces. Many experiments using different techniques have examined how cells respond to mechanical forces. Here, we focus on a simple geometry where the cell is between two plates. One of the plates is actuated vertically at velocity v, leading to an overall change in cell height, H (Fig. 4). Such an experiment was performed recently, where the cell adhesion areas at the two plates are fixed (20,42). This implies that there is negligible change in cell adhesion during pulling. We model the mechanics of the cell within this experiment. The goal is to explain changes in mechanical tension on the cantilever.

For a cylindrical cell, the cell volume and surface area are determined by the overall height, H, and cell radius, R.

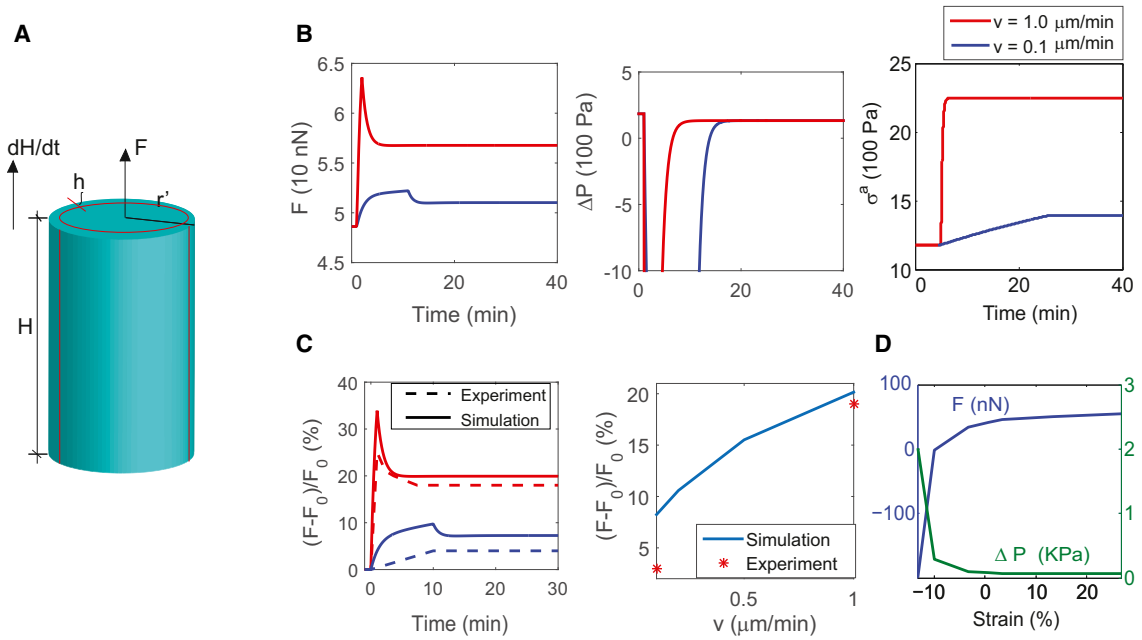

FIGURE 4 Cylindrical cell response to vertical displacements. (*A*) The vertical dimension of the cell, H, is changed at different velocities. The cortical thickness is h and the contact radius with the cantilevers is R. The model is used to compute the necessary pulling force, F. (*B*) As H is changed, the cell force response goes through several phases. Here, red and blue curves represent two different velocities of vertical displacement. The velocity of vertical displacement affects the transient force developed by the cell. If vertical displacement is fast, there is a large jump in force, because osmotic pressure and active stress cannot adapt quickly. The final steady-state force also depends on the displacement velocity. The final steady-state F depends on the rate of mechanical pulling, or strain rate. During pulling, the model also can compute the changes in cell osmotic pressure, ΔP, and the level of myosin active stress. (*C*) Comparisons of the model results with experimental results from Webster et al. (20). The final steady-state force agrees well with experimental results. The model can also fit a short-term transient force jump. (*D*) Model prediction of steady-state force as a function of vertical strain for a slow pulling case ($\sim 1\ \mu$ m/min). Curves at faster pulling rates are shown in Fig. 5. Note that the force is not zero at zero strain. Zero force is reached when the strain is $\sim -10\%$. To see this figure in color, go online.

During fast pulling or large strain, strictly speaking, the cell no longer maintains a cylindrical shape, and the cell radius will vary along the z direction (Fig. 4). The full geometry is mechanically complicated to analyze. For simplicity, we limit our discussion to the regime where the pulling rate is slower than the water permeation rate and approximate the cell as a cylinder throughout. The cell adhesion areas at the two plates are fixed, $z = 0$ and $z = H$. Therefore, we assume that R remains constant through the pulling/compressing process ($\partial R/\partial t \sim 0$). In this case, the volume change is simply related to a change in H, i.e., $\partial V/\partial t = \pi R^2 \partial H/\partial t$.

Under these assumptions and an active contractile stress of the form $\sigma_{\text{active}} = -\sigma^a(\mathbf{e_z}\otimes\mathbf{e_z} + \mathbf{e}_\theta\otimes\mathbf{e}_\theta)$, the membrane tension for a cylindrical cell under a constant force F at $z = H$ can be computed (see the Supporting Material for details) as

$$T = \left(\Delta P + \frac{F}{\pi R^2 - \pi(R-h)^2}\right)R - \sigma^a h\left(1+\frac{h}{R}\right)\left(1-\frac{h}{2R}\right), \tag{11}$$

where h is the cortical thickness. This result relies on the fact that h/H is a small parameter and the pulling velocity is slow, and therefore, the rate of cortical volume change is slow. We see that the membrane tension is again a combination of hydrostatic pressure, pulling force, cell dimensions, and active contractile stress.

Together with the constitutive relation in Eq. 10, water and ion permeation in Eq. 6, and biochemical regulation in Eq. 4, we again have a close set of equations. From these, we can predict how cells respond to external dimensional change and mechanical force, as well as osmotic changes.

Cell tension and step change in displacement

Some model results are shown in Fig. 4, where we compute the force response of the cell following the methods used in the experiments of Webster et al. (20). Direct comparisons between our model results and experimental data from Webster et al. (20) are shown in Fig. 4, *C* and *D*. We first apply a vertical displacement of 1.0 μm at $z = H$. This displacement is applied at different speeds, as illustrated in Fig. 4. We find that the force response of the cell depends on the rate of the external displacement. A faster displacement drives a stronger development of active contractile force. When a tensile displacement takes place, $\Delta\Pi$ decreases due to the volume expansion, which also changes

ΔP. Tension also increases from stretching in the membrane. These are the initial passive mechanical events upon a sudden tensile displacement. Subsequently, ions start to flow inside the cell (J_2) and myosin contraction becomes activated. This leads to contractile stress changes and adaptation of osmotic pressure. As the osmotic pressure difference recovers, the tensile force also decreases.

Our model shows features that are consistent with experiments on cell tension. When cells are pulled, the force jumps significantly but then recovers to a smaller value. The final steady-state force depends on the overall deformation and the strain rate, matching experimental results. As the strain becomes larger, the cell activates a larger portion of myosin in response to pulling and this force eventually saturates. However, the cell pressure is not dependent on strain rate and depends only on ion flux rates. The model also shows that in the negative strain direction, the cell adjusts osmotic pressure but generally resists compression. Here, active contraction does not play a significant role. In previous experimental studies, the cell was also subjected to a step-function-like displacement (with the strain rate approaching infinity), with the result that the final force is smaller than the final force when the pulling rate is smaller: 1 μ/min. Currently, our model does not predict such nonmonotonic strain response, because we assume that the cell maintains cylindrical shape and water permeation is fast.

Cell tension depends on cantilever stiffness

Remarkably, this model predicts that the cell should be sensitive to the stiffness of the cell environment. The following experiment can be modeled by our equations. A flexible cantilever is placed at one end of the cell and the cell is allowed to contract against it (Fig. 5). When the force exerted by the cell is equal to the cantilever force, $F = -K\Delta H$, where K is the cantilever stiffness, the system will reach mechanical equilibrium. Graphically, mechanical equilibrium is equivalent to the intersection of the F-versus- ΔH curve and $F = -K\Delta H$. The result shows that the cell contractile force increases with increasing cantilever stiffness. Experimental results from traction-force microscopy have shown a similar trend (1,43). Here, the cell volume and membrane tension are both higher when the cantilever is stiffer, and the cell exerts stronger contractile force to try to reduce volume and membrane tension. Note that adhesion in this problem is kept fixed, so cell adhesion changes do not play a role in our model.

In addition to cell tension, the steady-state cell volume also increases with cantilever stiffness (Fig. 5 *B*). These results suggest that while trying to maintain cell volume and membrane tension, the cell will exert forces that depend on the stiffness of the environment or the surrounding extracellular matrix. Although our model does not currently describe cells on a flat substrate, it is possible that the cell on flat surfaces may increase adhesions by spreading more broadly, thus increasing overall cell volume and membrane tension. Contractile forces are then increased to compensate for volume and tension changes. In addition, the strain-rate-dependent force response results in a different force-strain curve, as shown in Fig. 5 *B*. This adds a strain-rate-dependent dimension to the cell's response to changing cantilever stiffness (Fig. 5 *C*).

In addition, the model predicts that the steady-state amount of active myosin also depends on overall strain and the stiffness of the cantilever. The amount of myosin activation increases with increasing cantilever stiffness. With higher overall myosin activation and active tension in the cortex, the effective stiffness of the actin network in the cortex should be higher.

Cells during a step change in force

Figs. 4 and 5 show the cell response under a step change in displacement. Alternatively, one can apply a step change in force, and the results are shown in Fig. 6. Here, a jump in applied force of $F = 300$ nN is applied. The model predicts that the force jump leads to a rapid

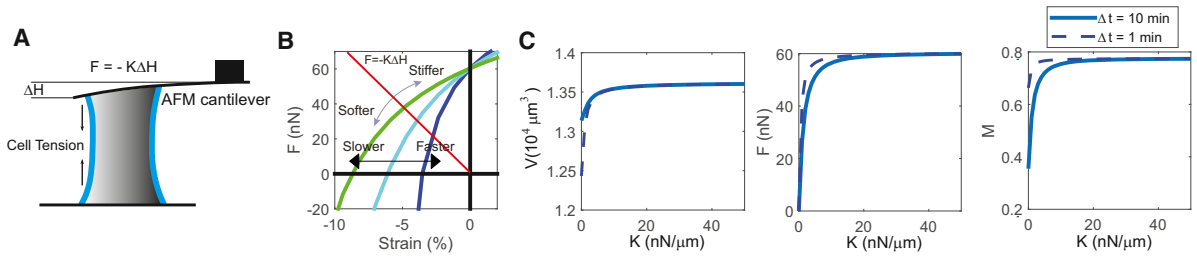

FIGURE 5 (*A*) A cell contracting against a flexible cantilever. The force of the cantilever is $F = -K\Delta H$, where K is the cantilever stiffness. (*B*) Mechanical equilibrium is reached when the cantilever force is equal to the cell contractile force. This represents the intersection between the F-versus-strain curve and $F = -K\Delta H$ (*red line*). Our model predictions for F versus strain are taken from Fig. 4 *D*. Different F-versus-strain curves represent results from different strain rates. Results show that the cell increases contractile force as K becomes larger (*green curve*). Here, for an adhesion radius of 20 μm, $K = 10$ nN/μm is equivalent to a Young's modulus of 500 Pa. (*C*) The model also predicts that cell volume is larger with a stiffer cantilever (*blue curve*). The contractile force generated by the cell also increases with increasing cantilever stiffness. This is because the activated form of myosin increases with increasing cantilever stiffness, which results from the increasing activation of Rho. To see this figure in color, go online.

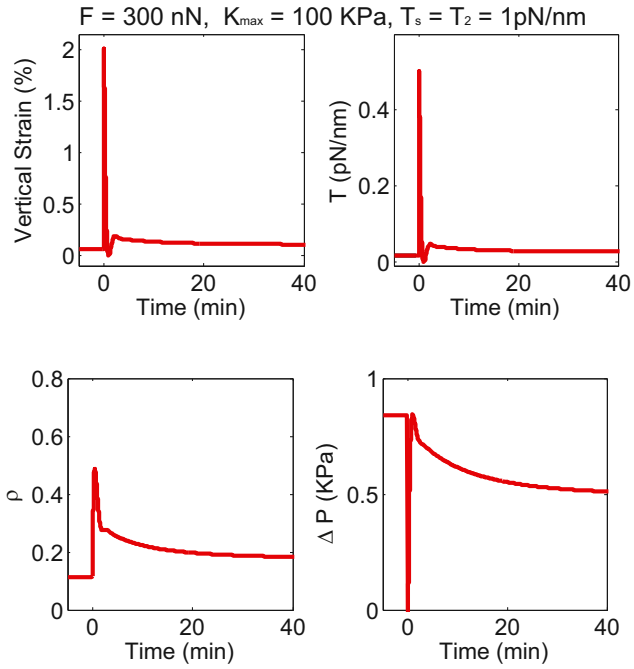

FIGURE 6 A cylindrical cell subjected to a jump in pulling force (300 nN) at $t = 0$ and K_{max} =100 kPa. The jump in applied force increases the activation of ρ and the active stress. The vertical strain therefore decreases slowly after a sudden increase. Water and ion flows also help to adjust the overall tension in the membrane. After a transient jump in pressure, tension, and Rho activation, the cell eventually recovers to the steady-state ρ and pressure. To see this figure in color, go online.

increase in membrane tension and lowering of osmotic pressure. This leads to activation of Rho and contraction. Concomitantly, the cell also adjusts the osmotic content, but this is slower. As the osmotic content rises, the contractile force falls and the membrane tension adjusts to close to its value before the force jump. The increase and decrease in Rho predicted by the model are in agreement with data from Zhao et al. (12), where cells were pulled by magnetic beads while the active form of Rho was measured. Note that our model assumes that water flow is relatively fast, and that the cell volume increases at the same rate as the force application. This is in general not realistic. Cell volume would slowly increase, which means that the initial jump in Rho activation should be slower. The full problem where water permeation rate is slow is complex and requires sophisticated computational approaches. It is beyond the scope of this article. Nevertheless, the model predicts an increase and subsequent decrease in Rho activation from cell osmotic adaptation. Also, notice that the intracellular pressure does not recover completely after application of force. This is because pressure at steady state is determined by osmolyte concentrate, and transient ion fluxes may lead to a lower steady-state osmotic pressure. In the Supporting Material, we discuss the influence of the ion channel and pump properties on pressure recovery.

DISCUSSION

Unlike plant and bacteria cells, animal cells lack a stiff outer cell wall to maintain their shape. Thus, active processes must compensate for changes in mechanical tension to maintain the cell shape and volume. Membrane tension and cell volume are both important for many cellular processes. Therefore, a key question is how these variables are maintained. In this article, we relate cell membrane and cortical tension to the osmotic pressure difference. We unify water and ion permeation, cell cortical mechanics, and myosin active contraction in a single model of cell mechanical and osmotic response, and we show that osmoregulation and regulation of myosin contraction can work together to maintain cell volume and membrane tension. Biochemical pathways that can adjust cell contractility have been identified. We study a model where membrane tension directly signals Rho activation and active contraction, and we show that such a model can maintain cell volume and membrane tension for a variety of environmental perturbations. Of course, other feedback mechanisms are possible. In particular, it has been noted that myosin II accumulation and contraction itself is tension-sensitive (13). Transient stress in the actin network may also activate Rho and myosin contraction. However, the actin cortex is highly dynamic and turns over quickly on a timescale of seconds. Sustained signaling from actin or myosin alone would require complex coordination. Nevertheless, it is possible multiple feedback mechanisms are at play, and further experiments are needed. Although details of the kinetics of the biochemical pathway are currently not available, we have used generic forms of activation and deactivation. Therefore, we expect qualitative agreement with experimental observations.

In this model, the cell membrane has a reference size, described by the constant A_0. This reference size is the equilibrium area of the membrane when there are no forces acting on it. It is determined by the total amount of lipid in the membrane and any possible thermal fluctuations that can generate folds. In the cell, A_0 is further regulated by lipid trafficking from the Golgi (44). If the membrane is under high tension, addition of lipid may become more likely than subtraction (41). Therefore, there is a third regulatory mechanism that controls A_0. Lipid trafficking, however, is likely quite slow, occurring on a timescale of hours, although rapid vesicle fusion has been observed in some situations (45). Therefore, in our current model, A_0 is assumed to be constant. It is also possible to develop a more comprehensive model incorporating dynamics of A_0. The actual quantitative predictions on homeostatic membrane tension depend on parameters such as T_c and T_s, and detailed measurements are needed to determine these parameters in MS channel activation.

In our model, we assume that the total protein content in the cell is constant and there is no active production of

osmolytes (described by n) in the cytoplasm. In a live cell during the G1 phase of the cell cycle, n of course changes due to transcription and translation, and the overall cell volume also increases. How the total protein content is controlled remains to be studied. There appear to be other signaling networks that control the total protein content, possibly by coupling to the active cell-volume control system. In addition, our model currently does not consider charges and voltage effects. This would require a more detailed model where Na, K, and Cl ions, and their respective channels, pumps, and exchangers are considered. This more detailed model requires other unknown parameters, and is beyond the scope of this article.

Results of our model show that a feedback control algorithm governing active cell contraction and osmotic regulation can maintain cell volume and control cellular force generation. Multiple feedback systems are potentially at play in maintaining cell volume and tension. Our model can be extended to consider cells at the multicellular tissue scale as well. At this larger scale, our model exhibits behaviors that are somewhat similar to those observed in the cellular Potts model used in tissue mechanics, although the details are not completely the same (46-48). In addition, with changes in parameters, the model can also exhibit oscillatory behavior (49). The missing model elements are signals that govern actin polymerization (through the Rac pathway) and signaling from cell adhesion. These elements are critical for understanding cell mechanics during migration and interaction with extracellular matrices. Cell adhesion and subsequent signaling affect both actin polymerization and myosin contraction. Once again, it is possible that membrane tension also plays a role. Experiments with beads have shown that integrin engagement alone can trigger actin polymerization (50). Modeling of these different pathways will yield new predictions about cell behavior in a wide variety of settings.

SUPPORTING MATERIAL

Supporting Materials and Methods, Supporting Results, six figures, and one table are available at http://www.biophysj.org/biophysj/supplemental/S0006-3495(15)00860-7

AUTHOR CONTRIBUTIONS

J.X.T. and S.X.S. designed the research, J.X.T. performed the research, and J.X.T. and S.X.S. wrote the article.

ACKNOWLEDGMENTS

The authors thank Sarita Korde and Florence Yellen for critical reading of the manuscript.

This work was supported by National Institutes of Health grants 1U54CA143868-01, 1R01GM075305 and NSF PHY-1205795.

REFERENCES

1. Discher, D. E., P. Janmey, and Y. L. Wang. 2005. Tissue cells feel and respond to the stiffness of their substrate. *Science.* 310:1139–1143.
2. Fraley, S. I., Y. Feng, …, D. Wirtz. 2010. A distinctive role for focal adhesion proteins in three-dimensional cell motility. *Nat. Cell Biol.* 12:598–604.
3. Bloom, R. J., J. P. George, …, D. Wirtz. 2008. Mapping local matrix remodeling induced by a migrating tumor cell using three-dimensional multiple-particle tracking. *Biophys. J.* 95:4077–4088.
4. Nelson, C. M., R. P. Jean, …, C. S. Chen. 2005. Emergent patterns of growth controlled by multicellular form and mechanics. *Proc. Natl. Acad. Sci. USA.* 102:11594–11599.
5. Stewart, M. P., J. Helenius, …, A. A. Hyman. 2011. Hydrostatic pressure and the actomyosin cortex drive mitotic cell rounding. *Nature.* 469:226–230.
6. Ingber, D. E. 2002. Mechanical signaling and the cellular response to extracellular matrix in angiogenesis and cardiovascular physiology. *Circ. Res.* 91:877–887.
7. Geiger, B., J. P. Spatz, and A. D. Bershadsky. 2009. Environmental sensing through focal adhesions. *Nat. Rev. Mol. Cell Biol.* 10:21–33.
8. Simões, Sde. M., J. T. Blankenship, …, J. A. Zallen. 2010. Rho-kinase directs Bazooka/Par-3 planar polarity during *Drosophila* axis elongation. *Dev. Cell.* 19:377–388.
9. Amano, M., K. Chihara, …, K. Kaibuchi. 1997. Formation of actin stress fibers and focal adhesions enhanced by Rho-kinase. *Science.* 275:1308–1311.
10. Jilkine, A., A. F. Marée, and L. Edelstein-Keshet. 2007. Mathematical model for spatial segregation of the Rho-family GTPases based on inhibitory crosstalk. *Bull. Math. Biol.* 69:1943–1978.
11. Maddox, A. S., and K. Burridge. 2003. RhoA is required for cortical retraction and rigidity during mitotic cell rounding. *J. Cell Biol.* 160:255–265.
12. Zhao, X. H., C. Laschinger, …, C. A. McCulloch. 2007. Force activates smooth muscle α-actin promoter activity through the Rho signaling pathway. *J. Cell Sci.* 120:1801–1809.
13. Luo, T., K. Mohan, …, D. N. Robinson. 2013. Molecular mechanisms of cellular mechanosensing. *Nat. Mater.* 12:1064–1071.
14. Fernandez-Gonzalez, R., Sde. M. Simoes, …, J. A. Zallen. 2009. Myosin II dynamics are regulated by tension in intercalating cells. *Dev. Cell.* 17:736–743.
15. Hoffmann, E. K., I. H. Lambert, and S. F. Pedersen. 2009. Physiology of cell volume regulation in vertebrates. *Physiol. Rev.* 89:193–277.
16. Sokabe, T., T. Fukumi-Tominaga, …, M. Tominaga. 2010. The TRPV4 channel contributes to intercellular junction formation in keratinocytes. *J. Biol. Chem.* 285:18749–18758.
17. Seminario-Vidal, L., S. F. Okada, …, E. R. Lazarowski. 2011. Rho signaling regulates pannexin 1-mediated ATP release from airway epithelia. *J. Biol. Chem.* 286:26277–26286.
18. Paré, A. C., A. Vichas, …, J. A. Zallen. 2014. A positional Toll receptor code directs convergent extension in *Drosophila*. *Nature.* 515:523–527.
19. Kolesnikov, T., and S. K. Beckendorf. 2007. 18 wheeler regulates apical constriction of salivary gland cells via the Rho-GTPase-signaling pathway. *Dev. Biol.* 307:53–61.
20. Webster, K. D., W. P. Ng, and D. A. Fletcher. 2014. Tensional homeostasis in single fibroblasts. *Biophys. J.* 107:146–155.
21. Chaudhuri, O., S. H. Parekh, …, D. A. Fletcher. 2009. Combined atomic force microscopy and side-view optical imaging for mechanical studies of cells. *Nat. Methods.* 6:383–387.
22. Joanny, J. F., and J. Prost. 2009. Active gels as a description of the actin-myosin cytoskeleton. *HFSP J.* 3:94–104.
23. Julicher, F., K. Kruse, …, J.-F. Joanny. 2007. Active behavior of the cytoskeleton. *Phys. Rep.* 449:3–28.

24. Mayer, M., M. Depken, …, S. W. Grill. 2010. Anisotropies in cortical tension reveal the physical basis of polarizing cortical flows. *Nature.* 467:617–621.
25. Jiang, H., and S. X. Sun. 2013. Cellular pressure and volume regulation and implications for cell mechanics. *Biophys. J.* 105:609–619.
26. Houk, A. R., A. Jilkine, …, O. D. Weiner. 2012. Membrane tension maintains cell polarity by confining signals to the leading edge during neutrophil migration. *Cell.* 148:175–188.
27. Pertz, O., L. Hodgson, …, K. M. Hahn. 2006. Spatiotemporal dynamics of RhoA activity in migrating cells. *Nature.* 440:1069–1072.
28. Tkachenko, E., M. Sabouri-Ghomi, …, M. H. Ginsberg. 2011. Protein kinase A governs a RhoA-RhoGDI protrusion-retraction pacemaker in migrating cells. *Nat. Cell Biol.* 13:660–667.
29. Clark, A. G., K. Dierkes, and E. K. Paluch. 2013. Monitoring actin cortex thickness in live cells. *Biophys. J.* 105:570–580.
30. Luo, T., K. Mohan, …, D. N. Robinson. 2012. Understanding the cooperative interaction between myosin II and actin cross-linkers mediated by actin filaments during mechanosensation. *Biophys. J.* 102:238–247.
31. Joanny, J.-F., K. Kruse, …, S. Ramaswamy. 2013. The actin cortex as an active wetting layer. *Eur. Phys. J. E. Soft Matter.* 36:52.
32. Fernandez-Gonzalez, R., and J. A. Zallen. 2009. Cell mechanics and feedback regulation of actomyosin networks. *Sci. Signal.* 2:pe78.
33. Matthews, B. D., D. R. Overby, …, D. E. Ingber. 2006. Cellular adaptation to mechanical stress: role of integrins, Rho, cytoskeletal tension and mechanosensitive ion channels. *J. Cell Sci.* 119:508–518.
34. Salbreux, G., J. F. Joanny, …, P. Pullarkat. 2007. Shape oscillations of non-adhering fibroblast cells. *Phys. Biol.* 4:268–284.
35. Gao, J., R. T. Mathias, …, G. J. Baldo. 1995. Two functionally different Na/K pumps in cardiac ventricular myocytes. *J. Gen. Physiol.* 106:995–1030.
36. Armstrong, C. M. 2003. The Na/K pump, Cl ion, and osmotic stabilization of cells. *Proc. Natl. Acad. Sci. USA.* 100:6257–6262.
37. Safran, S. A. 1994. Statistical Thermodynamics of Surfaces, Interfaces, and Membranes. Addison-Wesley, Reading, MA.
38. Upadhyaya, A., and M. P. Sheetz. 2004. Tension in tubulovesicular networks of Golgi and endoplasmic reticulum membranes. *Biophys. J.* 86:2923–2928.
39. Alberts, B., A. Johnson, …, P. Walter. 2002. Molecular biology of the cell, 4th edition. Garland Science, New York, Chapter 13, Intracellular Vesicular Traffic. 711–766.
40. Peliti, L., and S. Leibler. 1985. Effects of thermal fluctuations on systems with small surface tension. *Phys. Rev. Lett.* 54:1690–1693.
41. Sens, P., and M. S. Turner. 2006. Budded membrane microdomains as tension regulators. *Phys. Rev. E Stat. Nonlin. Soft Matter Phys.* 73:031918.
42. Webster, K. D., A. Crow, and D. A. Fletcher. 2011. An AFM-based stiffness clamp for dynamic control of rigidity. *PLoS One.* 6:e17807.
43. Lo, C. M., H. B. Wang, …, Y. L. Wang. 2000. Cell movement is guided by the rigidity of the substrate. *Biophys. J.* 79:144–152.
44. Tang, Q., and M. Edidin. 2001. Vesicle trafficking and cell surface membrane patchiness. *Biophys. J.* 81:196–203.
45. Groulx, N., F. Boudreault, …, R. Grygorczyk. 2006. Membrane reserves and hypotonic cell swelling. *J. Membr. Biol.* 214:43–56.
46. Maree, A. F. M., V. A. Geieneisen, and P. Hogeweg. 2007. The cellular potts model and biophysical properties of cells, tissues and morphogenesis. *In* Single-Cell-Based Models in Biology and Medicine. Birkhauser Verlag, Basel, Switzerland, pp. 77–78.
47. Honda, H. 1978. Description of cellular patterns by Dirichlet domains: the two-dimensional case. *J. Theor. Biol.* 72:523–543.
48. Farhadifar, R., J.-C. Röper, …, F. Jülicher. 2007. The influence of cell mechanics, cell-cell interactions, and proliferation on epithelial packing. *Curr. Biol.* 17:2095–2104.
49. Koride, S., L. He, …, S. X. Sun. 2014. Mechanochemical regulation of oscillatory follicle cell dynamics in the developing *Drosophila* egg chamber. *Mol. Biol. Cell.* 25:3709–3716.
50. Bun, P., J. Liu, …, M. Coppey-Moisan. 2014. Mechanical checkpoint for persistent cell polarization in adhesion-naive fibroblasts. *Biophys. J.* 107:324–335.

Active Biochemical Regulation of Cell Volume and a Simple Model of Cell Tension Response: Supplemental Material

Jiaxiang Tao and Sean X. Sun[1]

[1] *Department of Mechanical Engineering, Biomedical Engineering and Johns Hopkins Physical Sciences-Oncology Center, Johns Hopkins University, Baltimore, MD 21218, USA*

I. FORCE BALANCE AT THE CELL SURFACE

At the cell membrane, let us consider a surface element S bounded by contour c with its unit tangent vector, $\mathbf{t}$, going counter-clockwise. $\mathbf{n}$ is a unit normal vector, perpendicular to $\mathbf{t}$, and $\mathbf{m}$ is orthogonal to both $\mathbf{t}$ and $\mathbf{n}$. (as shown in Fig. 1). If the membrane surface has a tension T, then the total force on the region bounded by c arising from tension is

$$\mathbf{F_c} = \int_c T\mathbf{m}dl \tag{1}$$

where dl is a line element of the contour c (Fig. 1). From Fig. 1, we have $\mathbf{m} = -\mathbf{n} \times \mathbf{t}$. The net force acting on the membrane surface then is: $\mathbf{F_c} = -\int_c (T\mathbf{n} \times \mathbf{t})\, dl$.

If we integrate an arbitrary vector field $\mathbf{a} \times \mathbf{b}$ on the closed contour c, where $\mathbf{b}$ is a constant vector field, according to Stoke's theorem, we have

$$\int_c (\mathbf{a} \times \mathbf{b}) \cdot \mathbf{t}dl = \int_S (\nabla \times (\mathbf{a} \times \mathbf{b})) \cdot \mathbf{n}dS \tag{2}$$

The left-hand side of the Eq. 2 can be transformed as: $\int_c (\mathbf{a} \times \mathbf{b}) \cdot \mathbf{t}dl = \int_c -\mathbf{b} \cdot (\mathbf{a} \times \mathbf{t})dl$. We can then use the identity: $(\nabla \times (\mathbf{a} \times \mathbf{b})) = \mathbf{b} \cdot \nabla\mathbf{a} - \mathbf{b}(\nabla \cdot \mathbf{a})$ to modify the right hand of Eq. 2. Then, after canceling out the constant vector $\mathbf{b}$, we obtain: $-\int_c (\mathbf{a} \times \mathbf{t})\, dl = \int_S (\mathbf{n} \cdot \nabla\mathbf{a} - \mathbf{n}(\nabla \cdot \mathbf{a}))\, dS$. Comparing this to Eq. 1, and set $\mathbf{a} = T\mathbf{n}$, we have:

$$\mathbf{F_c} = \int_S -T\mathbf{n}(\nabla \cdot \mathbf{n}) + \nabla T dS \tag{3}$$

This relationship shows that there is a net force that acts perpendicular to the boundary of C, and is proportional to the local mean curvature, C, because $\nabla \cdot \mathbf{n} = 2C$. If the tension is a constant and the surface is flat, the line integral will be zero.

At equilibrium, the force from tension must be balanced by other forces acting on the membrane. The total force on the surface by regions above and below the interface is

$$\mathbf{F_f} = \int_S \mathbf{n} \cdot \sigma_2|_S - \mathbf{n} \cdot \sigma_1|_S\, dS \tag{4}$$

where σ_1 denotes stress in extracellular fluid (above the membrane in Fig. 1(a)) and σ_2 denotes stress in the intracellular region below the membrane. $|_S$ denotes the values at the membrane surface. This force jump condition is a fundamental property of interfaces and does not depend on material properties. In our following discussion, we generally assume that there is no stress in the extracellular region ($\sigma_1 = 0$). For the intracellular region below the membrane, we will consider the dynamics within the actomyosin cortex and stresses arising from it.

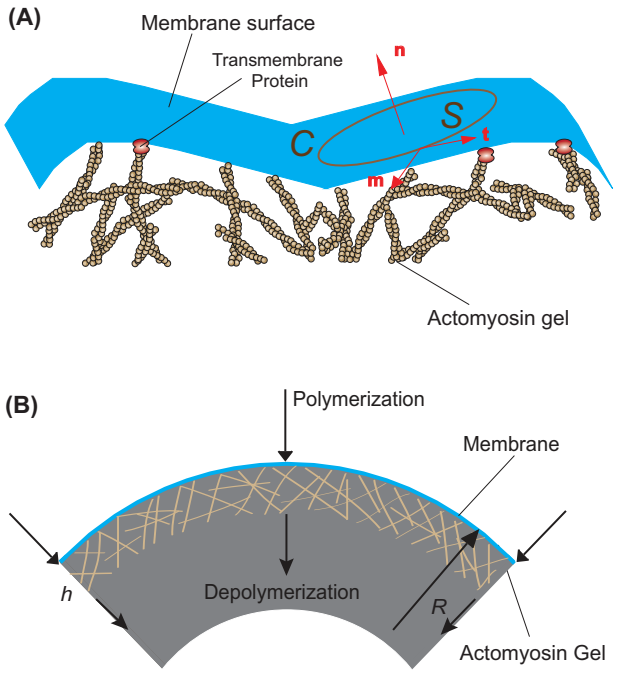

FIG. 1. The membrane and the actomyosin cortex in a living cell. (A): A typical picture of the membrane surface (blue) which is adhered to actin filaments through transmembrane proteins such as formins (red inserts). We consider the membrane as a single fluid layer (blue) and the actomoysin cortex is modeled as a fluid gel. For the force balance consideration, vectors $\mathbf{t}$, $\mathbf{n}$, and $\mathbf{n}$ are defined around a surface element S with contour c. (B) A spherically symmetric cell surface element: the local radius of curvature is R and the cortical thickness is h. Actin polymerization takes place at $r = R$ and depolymerization takes place at $r = R - h$. Within the cortex, there is also an active contractile stress σ^a.

At mechanical equilibrium, $\mathbf{F_f} + \mathbf{F_c} = 0$. Therefore, applying Eqs. (1) and (4), force balance along the normal and tangential directions gives, respectively:

$$\begin{aligned} T(\nabla \cdot \mathbf{n}) &= \mathbf{n} \cdot \sigma_2|_S \cdot \mathbf{n} \\ (\nabla T) \cdot \mathbf{t} &= -\mathbf{t} \cdot \sigma_2|_S \cdot \mathbf{n} \end{aligned} \tag{5}$$

Eq. (5) is subject to modification if extra body forces are presented at the interface. For example, the hydrostatic pressure difference, ΔP, which is equal to the osmotic pressure difference at steady volume across the membrane will add an additional normal force term in Eq. (5), i.e.,

$$T(\nabla \cdot \mathbf{n}) = \mathbf{n} \cdot \sigma_2|_S \cdot \mathbf{n} + \Delta P \mathbf{n} \tag{6}$$

Tangential force balance in Eq. (5) suggests that net tangential force is balanced by gradients in the tension. If a non-uniform membrane tension is present, the line integral at Eq. (1) will produce a net force that is along the $\mathbf{t}$ direction. This net force at equilibrium should be balanced by external forces acting on the interface, such as coming from a lipid tether.

II. TENSION EXPRESSIONS

We now consider a simple active gel model and treat the actin cortex as Newtonian incompressible fluid, the mechanical stress in the cortex is then:

$$\sigma_2 = \sigma_p + \sigma_{active} = \underbrace{-p\mathbf{I} + 2\mu\big(\nabla \mathbf{u} + \nabla \mathbf{u}^{\mathbf{T}}\big)}_{\sigma_p} + \sigma_{active} \tag{7}$$

where p is the pressure in the cortex; $\mathbf{u}$ is the actin flow velocity. σ_{active} is the active contractile stress from myosin, which acts tangential to the cell surface.

Spherical Cell

For a mitotic cell or a cell in suspension, the cell shape is spherical and the cytoskeletal flow is mainly along the radial direction. Therefore, the velocity field of the actomyosin cortex, $\mathbf{u}$, is only a function of r, i.e. $\partial_\theta u_i = 0$ and $\partial_\phi u_i = 0$. Because of the axisymmetric assumption: $u_\theta = u_\phi = 0$. The continuity equation for an incompressible fluid is $\nabla \cdot \mathbf{u} = 0$. The net mass of the cortex is also not changing, and polymerization at the membrane equals depolymerization. In spherical coordinates, continuity equation is then:

$$\frac{1}{r^2}\frac{\partial}{\partial r}\left(r^2 u_r\right) = 0 \tag{8}$$

At the membrane-cortex interface, the boundary conditions is $u_r(r = R) = U$, where U is the material velocity from polymerization at $r = R$. Therefore, the velocity field is:

$$u_r = U\frac{R^2}{r^2} \tag{9}$$

If we assume isotropic active contraction stress: $\sigma_{active} = -\sigma^a\left(\mathbf{e}_\theta \otimes \mathbf{e}_\theta + \mathbf{e}_\phi \otimes \mathbf{e}_\phi\right)$, then the r-component of Stoke's equation for spherical incompressible actomyosin fluid is:

$$-\frac{\partial p}{\partial r} + \mu\left[\frac{1}{r^2}\frac{\partial}{\partial r}\left(r^2\frac{\partial u_r}{\partial r}\right) - 2\frac{u_r}{r^2}\right] + \frac{2\sigma^a}{r} = 0 \tag{10}$$

Solving the pressure from Eq. 10 gives:

$$p = p(r = R - h) - 2\sigma^a \ln\left[\frac{R-h}{r}\right] \tag{11}$$

where $p(r = R - h)$ is the pressure boundary condition at $r = R - h$. We assume $\mathbf{n} \cdot \sigma_2(r = R - h) \cdot \mathbf{n} = 0$. This gives $p(r = R - h)$. Also, since $h \ll R$, the stress exerted by the cortex on the membrane, σ_2, is approximately:

$$\mathbf{n} \cdot \sigma_2(r = R) \cdot \mathbf{n} \sim 4\mu U\left[\frac{1}{R-2h} - \frac{1}{R}\right] - \frac{2\sigma^a h}{R} \tag{12}$$

The total force acting at membrane is then: $\mathbf{n} \cdot \boldsymbol{\sigma_2}(r = R) \cdot \mathbf{n} + \Delta P$. Substitute Eq. 12 into Eq. 6, we have

$$\frac{2T}{R} \sim 4\mu U\left[\frac{1}{R-2h} - \frac{1}{R}\right] + \Delta P - 2\sigma^a\frac{h}{R} \tag{13}$$

For a typical suspended cell, the hydrostatic pressure difference across the membrane is in the order of 0.5 to 1 kPa[1, 2]. The viscosity of actin network is $\mu \sim 0.01 - 1$Pa.s [3]. The actin polymerization velocity, U, is approximately 0.01-1μm/s [4]. Let us compare terms in Eq. (13): the hydrostatic pressure contribution is of similar order of magnitude as the active stress term. The viscous term, $\mu U R^2\left(\frac{1}{(R-h)^3} - \frac{1}{R^3}\right)$, is $\sim 10^{-3}$ Pa, which is expected to be much smaller than the hydrostatic pressure and active stress term. Thus, we can ignore the viscous flow in our calculation, resulting expression in Eq. 4 in the main text.

Cylindrical Cell under Mechanical Force

For the cylindrical geometry in Fig. 4 of the main text, we assume the active contractile stress is of the form:

$$\sigma_{active} = -\sigma_1^a \mathbf{e_z} \otimes \mathbf{e_z} - \sigma_2^a \mathbf{e}_\theta \otimes \mathbf{e}_\theta \tag{14}$$

The active force is:

$$\nabla \cdot \sigma_{active} = \frac{\sigma_2^a}{r}\mathbf{e_r} - \frac{\partial \sigma_1^a}{\partial z}\mathbf{e_z} \tag{15}$$

We again assume the actomyosin gel behaves as incompressible Newtonian fluid, where the passive stress is described by Eq. 7:

If we assume the system is cylindrically symmetric, the actin flow velocity is: $\mathbf{u} = u_r\mathbf{e_r} + u_z\mathbf{e_z}$ and $\frac{\partial \cdots}{\partial \theta} = 0$.

To solve the full expression of actin flow velocity, we need boundary conditions. They are as follows:

$$\begin{aligned} u_z(z=0) &= 0 \\ u_z(z=H) &= \frac{dH}{dt} \\ \mathbf{n}\cdot\sigma_{\mathbf{2}}|_{z=H}\cdot\mathbf{n} &= \frac{F}{\pi(R^2-(R-h)^2)}+\Delta P \\ u_z(r=R) &= 0 \\ \mathbf{n}\cdot\sigma_{\mathbf{2}}|_{r=R-h}\cdot\mathbf{t} &= 0 \end{aligned} \tag{16}$$

where $\mathbf{n}$ is the unit normal vector for the membrane surface. At the cylinder surface, $\mathbf{n}=\mathbf{e_r}$, and at the top surface, $\mathbf{n}=\mathbf{e_z}$. $\mathbf{t}$ is the unit tangent vector, perpendicular to $\mathbf{n}$. Because we assume cylindrical symmetry, $\mathbf{t}=\mathbf{e_z}$ at the cylinder surface. $\pi R^2-\pi\left(R-h\right)^2$ is the contact area where the force is applied, and we assume that the force is applied to the cytoskeleton region, where the cell is adhered to the cantilever.

The Stokes equation in this case is again

$$\nabla\cdot(\sigma_p+\sigma_{active})=0 \tag{17}$$

where the expression for $\nabla\cdot\sigma_{active}$ is given in Eq. 15, and:

$$\begin{aligned}(\nabla\cdot\sigma_p) = &\left[-\frac{\partial p}{\partial r}+4\mu\left[\frac{\partial^2 u_r}{\partial r^2}+\frac{1}{r}\left(\frac{\partial u_r}{\partial r}-\frac{u_r}{r}\right)+\frac{\partial^2 u_r}{\partial z^2}\right]\right]\mathbf{e_r} \\ &+\left[-\frac{\partial p}{\partial z}+4\mu\left[\frac{\partial^2 u_z}{\partial z^2}+\frac{1}{2}\left(\frac{\partial}{\partial r}+\frac{1}{r}\right)\left(\frac{\partial u_r}{\partial z}+\frac{\partial u_z}{\partial r}\right)\right]\right]\mathbf{e_z}\end{aligned} \tag{18}$$

Solving Eq. 17 is complicated. But we will use expansions to give analytic estimates for tension. In particular, it is clear that the thickness of the cortex is small when compared to other dimensions of the system, i.e., $h\ll(H,R)$. This implies that $h/H\sim 500\text{nm}/20\mu\text{m}\sim 0.02$ is a small parameter and any terms scaled by (h/H) or higher can be neglected. During pulling, assuming actin polymerization is fast and cortical thickness is constant, the continuity equation implies

$$\nabla\cdot\mathbf{u}\sim\frac{1}{H}\frac{dH}{dt}=\frac{v}{H} \tag{19}$$

which is assumed to be small. Also, since $u_r\sim U$ and $\partial u_r/\partial r\sim u_r/h$, and $\partial u_z/\partial z\sim u_z/H$, we have $u_r\sim h/Hu_z$. With this approximation, we can examine the relative magnitude of each term in Eq. 17. For the z-component of force balance, we have approximately $\frac{\partial^2 u_z}{\partial z^2}\sim\left(\frac{\partial}{\partial r}+\frac{1}{r}\right)\frac{\partial u_r}{\partial z}\sim\frac{u_z}{H^2}$, while $\left(\frac{\partial}{\partial r}+\frac{1}{r}\right)\frac{\partial u_z}{\partial r}\sim u_z/h^2$. Thus, $\frac{\partial^2 u_z}{\partial z^2}$ and$\left(\frac{\partial}{\partial r}+\frac{1}{r}\right)\frac{\partial u_r}{\partial z}$ are small when compared to $\left(\frac{\partial}{\partial r}+\frac{1}{r}\right)\frac{\partial u_z}{\partial r}$. The z-component of Eq. 17 is simplified to

$$-\frac{\partial p}{\partial z}+\underbrace{2\mu\left(\frac{\partial}{\partial r}+\frac{1}{r}\right)\frac{\partial u_z}{\partial r}}_{\sim 2\mu u_z/h^2}-\frac{\partial\sigma_1^a}{\partial z}=0 \tag{20}$$

In order for the active contraction term to be comparable to the viscous term, $\partial\sigma_1^a/\partial z\sim\sigma_1^a/H$ has to be at least in the order of $2\mu u_z/h^2$. The viscous term of the r-component of Eq. 17 is in the order of $\mu u_z/(hH)$, and $\sigma_2^a\sim\sigma_1^a$. Therefore, σ_2^a/r is in the order of $2\mu u_z/h^2$, the active contraction term in the r-component equation is much larger than the viscous term. Therefore, the r-component can be simply written as:

$$-\frac{\partial p}{\partial r}+\frac{\sigma_2^a}{r}=0 \tag{21}$$

which gives: $p=p_0(z)+\sigma_2^a\ln\left(\frac{r}{R-h}\right)$.

Substituting Eq. 21 back to Eq. 20, we can solve for $\partial u_z/\partial r$. We obtain

$$r\frac{\partial u_z}{\partial r}=\frac{r^2-(R-h)^2}{4\mu}\frac{\partial}{\partial z}(p+\sigma_1^a) \tag{22}$$

Using the no stress at $R-h$ boundary condition described in Eq. 16, evaluating Eq. 22 at $r=R$, we have

$$\mathbf{n}\cdot\sigma_{\mathbf{2}}\cdot\mathbf{t}|_{r=R}=2\mu\frac{\partial u_z}{\partial r}|_{r=R}=\frac{1}{2}\left(R-\frac{(R-h)^2}{R}\right)\frac{\partial}{\partial z}\left(p+\sigma_1^a\right) \tag{23}$$

Since $h\ll R$, the pressure field is approximately $p=p_0+\sigma_2^a\frac{h}{R}$.

Given the stress field in the cortex, there are in principle two ways to solve for tension . One is from normal force balance: $-T(\nabla\cdot\mathbf{n})-\mathbf{n}\cdot\sigma_2|_S\cdot\mathbf{n}-\Delta P\mathbf{n}=0$, the other is from tangential force balance: $\nabla T+\mathbf{n}\cdot\sigma_{\mathbf{2}}\cdot\mathbf{t}|_{r=R}=0$. We just obtained $\mathbf{n}\cdot\sigma_{\mathbf{2}}\cdot\mathbf{t}|_{r=R}$, therefore we can use tangential force balance to solve for the tension gradient. Integrating Eq. 23 over z, we have for the tension

$$T=T_0-\frac{1}{2}\left(R-\frac{(R-h)^2}{R}\right)\left(\sigma_2^a\frac{h}{R}+\sigma_1^a\right) \tag{24}$$

Applying the boundary condition from Eq. 16: $-T_0(\nabla\cdot\mathbf{n})+\mathbf{n}\cdot\sigma_2|_{z=H}\cdot\mathbf{n}+\Delta P=0$, we find $T_0=\left(\Delta P+\frac{F}{\pi R^2-\pi(R-h)^2}\right)R$.

We notice that the contribution for the circumferential component of active contraction is of the order of h/R times the axial contraction contribution. Thus, if $\sigma_1^a=\sigma_2^a=\sigma^a$, the contribution from tangential component of active contraction is smaller than the axial component contribution. If the active stress is isotropic, then the tension expression can be further simplified to:

$$\begin{aligned}T=&\left(\Delta P+\frac{F}{\pi R^2-\pi(R-h)^2}\right)R \\ &-\sigma^a h\left(1+\frac{h}{R}\right)\left(1-\frac{1}{2}\frac{h}{R}\right)\end{aligned} \tag{25}$$

which is the expression in Eq. 10 in the main text.

We may notice that the approximate solution for the flow field we purposed does not satisfy all boundary conditions shown in Eq. 16. The flow field has to be independent of r when $z=H$, while our flow velocity expression

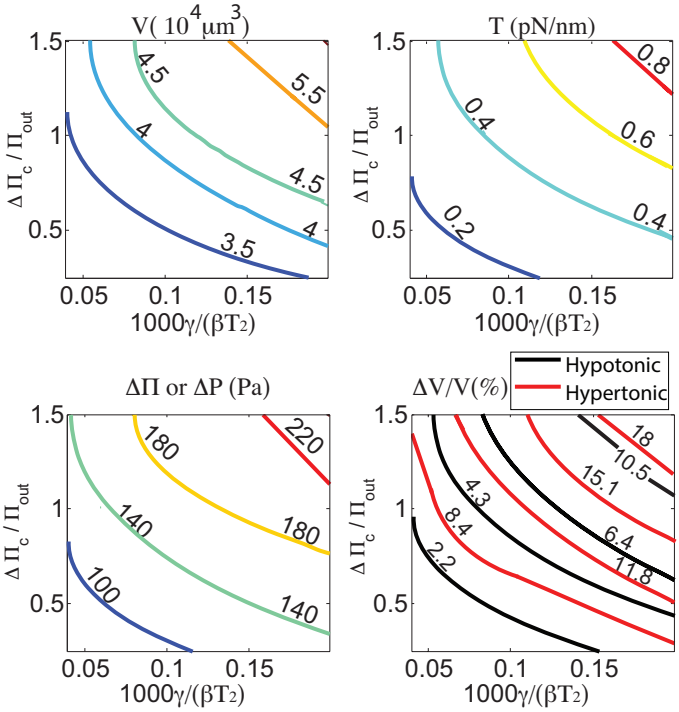

FIG. 2. Contour plots of steady state behavior of the cell after a 0.2 MPa hypo/hypertonic shock. Labels indicate values of contours. Two critical parameters $\gamma/\beta T_2$ and $\Delta\Pi_c/\Pi_{out}$ determine the steady state behavior. The contour plots for cell volume, membrane tension, ΔPi which is equal to ΔP at steady state, and percent change in volume after the shock (Δ/V are plotted as a function of $\gamma/\beta T_2$ and $\Delta\Pi_c/\Pi_{out}$. The contours values are labeled.

does not have that property. This is because we assume the z dependence of flow field is weak and, therefore, can be ignored. A simple estimate can demonstrate that this is a reasonable approximation. From basic physics of pipe flow, the fluid "enters" a cylindrical region with uniform velocity field, and, due to the non-slip boundary condition, fully develops into a parabolic distribution within certain length scale. To analytically solve the full fluid equation from $z = 0$ to $z = H$ is difficult, but if the "entrance" or "exist" effect is small, derivation shown above can still be valid for most of the cell.

The entrance or the exit length is defined as the length-scale at which the flow develops from a uniform flow field to a parabolic distribution, or, from $u_z = v$ to $\frac{\partial u_z}{\partial z} \sim 0$. The order of magnitude for entrance length is: $L_e = \frac{A}{L_0}$; in which A is the cross sectional area and L_0 is the "wet perimeter of the pipe". In this case: $A = \pi\left[R^2 - (R-h)^2\right] \sim 2\pi Rh$ when $h << R$; and $L_0 \sim 2\pi R + 2\pi(R-h)$. Thus, entrance length is: $L_e \sim \frac{Rh}{2R-h}$. Substituting $h = 0.5\mu$m; $R \sim 20\mu$m, we have: $L_e \sim 0.25\mu$m. If $H \sim 10$ to 20μm, the entrance/exit length is in the order of 1 to 2% of the total cell height, H. This means, the flow field we estimated above works for over 95% of the cell length. The tension expression in Eq. 25 is, therefore, a valid estimation. This consideration also suggests that complex stress distributions exist at the ends of the cell in this geometry.

III. ADDITIONAL RESULTS ON ADAPTATION TO OSMOTIC SHOCK

In the main text, we showed that both ion flux and Rho signaling network are important for cells to adapt to osmotic shocks. The Rho signaling network controls myosin contraction [5], which limits volume change, and ion fluxes adjust pressure differences across the membrane. Both factors influence cell cortical tension, myosin activation and ion channel opening. In this section, we will discuss the steady state behavior of the cell after osmotic shocks in terms of two dimensionless parameters: $\frac{1000\gamma}{\beta T_2}$ and $\frac{\Delta\Pi_c}{\Pi_{out}}$.

T_2 is the saturating membrane tension for the mechanosensitive (MS) ion channels, and therefore βT_2 describes the maximum ion flux through the MS ion channel for a given osmotic pressure difference across the membrane. $\frac{\gamma}{\beta T_2}$ is a parameter describing flux ratio through ion pumps and MS channels. Also notice that $\Delta\Pi_c$ is in the order of Π_{out} ($0.1\sim$ 1 MPa); $\Delta\Pi$ is in the order of 100 Pa (10^{-4} MPa) [1], and T_2 is in the order of 1 pN/nm. Thus, in order for J_1 to be similar in magnitude as J_2, such as when the cell is in steady state, γ has to be approximately 1,000 times smaller than βT_2.

As described in the main text, the ion pump performance is determined by $\Delta\Pi_c$, which is proportional to Π_{out}. The ratio $\Delta\Pi_c/\Pi_{out}$ is related to ΔG_a, the free energy available for the pump. In Fig. 2, we see that a larger ratio $\Delta\Pi_c/\Pi_{out}$ will result in larger cell volume, tension, pressure differences and permanent volume changes after the shock, while the MS channels help to relieve excess pressure. In our model, we try to keep the post-shock permanent volume change below 10 % of pre-shock volume, which subsequently result in steady state tension in the order of 0.5 pN/nm and pressure differences around 160 to 200 Pa. We also find that at the same shock magnitude, cell recovers better after hypotonic shock than after hypertonic shock. This is because the increasing in tension during hypotonic shock brings myosin contraction into volume adaptation, while for hypertonic shock, the adaptation mainly comes from passive ion flux.

Additionally, our model predicts that if there is a constant increase in solutes in the cell, such from production of proteins, the volume also increases in order to keep a constant solute concentration inside the cell, so that the osmotic pressure inside the cell is a constant. As a consequence, higher solute content results in higher membrane tension and higher myosin activity, as shown in Fig. 3. However, if lipid trafficking is incorporated in our model, increases in n may trigger more incorporation

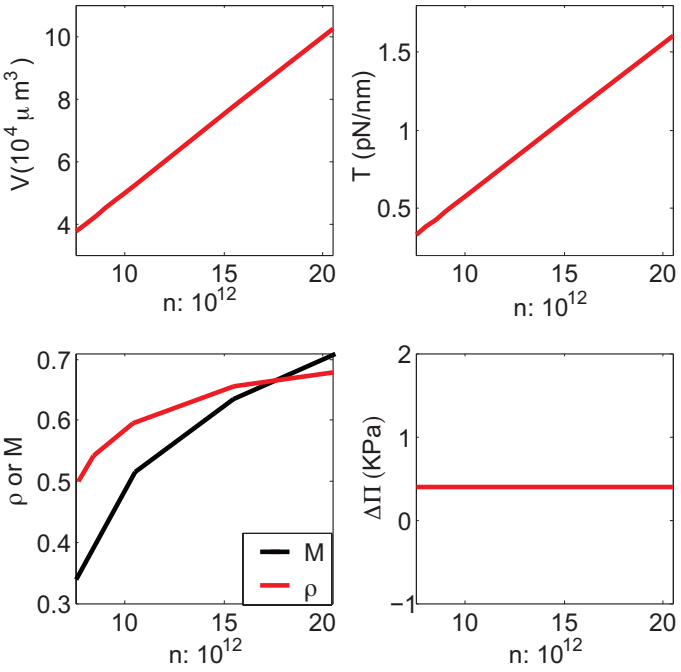

FIG. 3. Cell volume as a function of the total protein content in the cell. Our model predicts that the cell keeps a constant solute concentration, and increase volume to maintain this concentration. Assuming that everything else remains constant, membrane tension also increases with increasing solute content. Myosin contractile activity is also higher for a cell with larger solute content.

of lipid from the ER, and the membrane tension may still remain relatively constant throughout. Also, the numerical value of the constant concentration is determined by parameters such as K_{max} and flux parameters. This result suggest that cells may use this system to sense the concentration of its important proteins.

TRANSIENT STRESS

As we mentioned in the main text, experimental results demonstrated that there is a sudden change in cytoskeleton structure when the cell is subjected to a high strain rate. α-actinin crosslinker has been shown to be involved in determining post-pulling cell tension during vertical displacement experiments [6, 7]. These studies also showed that over-expressing α-actinin results in higher cell force response. Mechanically, cross linking proteins in the actin network change the shear modulus, μ, of the actin network. For the same deformation, a strongly cross linked network with a larger μ will result in higher mechanical stress in the network.

In our model, we describe two independent mechanisms of myosin activation: Rho signal network-related myosin activation and transient-force related myosin activation. The second mechanism describes the fact that binding and unbinding to actin by myosin depend on the load on the actin filament [8]. We simulate such effects by changing in myosin activation rate, a_2. We assume that a higher transient shear stress will promote myosin activation.

For highly viscous Newtonian flow, the cortical flow field can be approximated by a linear combination of actin flow from active contraction, and the non-steady state viscous shear flow due to the moving boundary at $z = H$. The non-steady, viscous shear flow is on the same order as the boundary velocity. To solve for the full cortical flow field with the moving boundary is difficult. However, we can do the same scaling analysis to estimate the shear stress in the cortex during pulling. Using the moving boundary at $z = H$, the maximum velocity for the actin flow should be in the order of $\frac{dH}{dt}$, which we defined as v. Similar force boundary condition (no-slip at $r = R$; stress-free at $r = R - h$) is described in Eq. 16. The transient actin flow velocity field along the z direction is in the order of:

$$u_z = v\left[1 - \left(\frac{r-(R-h)}{h}\right)^2\right] \tag{26}$$

which gives the viscous stress at $z = h$: $\sigma_p = 2\mu\frac{\partial u_z}{\partial r}|_{z=h}$, or

$$\sigma_p = 4\mu\frac{v}{h} \tag{27}$$

where μ is cortical viscosity, which is in the order of 10^{-5} pN/nm^2·s. This means, if v is in the order of 10 μm per min, the transient viscous stress is significant. Thus, the total viscous force acting on the membrane-cytoskeleton area per unit membrane length is

$$T_{shear} = \sigma_p H = 4\mu v\frac{H}{h} \tag{28}$$

Eq. (28) describes the relationship between transient shear stress and strain rate. Using this relationship, we can write the dimensionless activation function, f, in Eq. 5 in the main text as:

$$f = \frac{T_{shear}}{T_r} \tag{29}$$

where T_r is a scale parameter, in units of force per length, representing the tension scale above which shear stress will have a significant effect on myosin activation and force generation. A similar model can be made for the myosin disassembly rate d_2. One can develop more complex models by incorporating realistic molecular response of myosin mini-filaments. However, the molecular details are not available currently and therefore a simple model is used to demonstrate its predictions.

This model also incorporates possible effects of actin cross linkers because changes in cross linker density leads

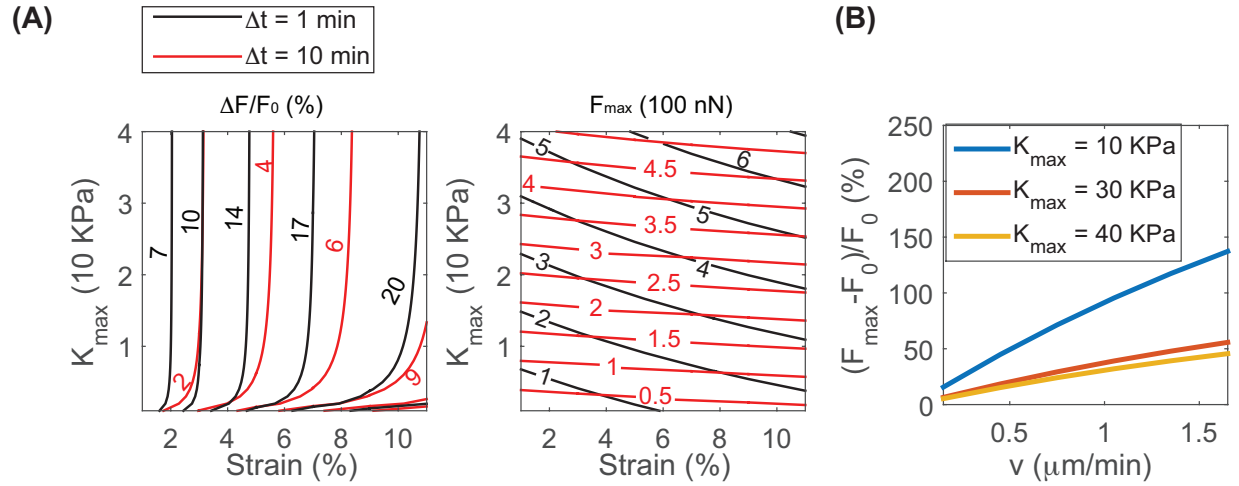

FIG. 4. Model results for cylindrical cell force response after vertical deformation. (A) Steady state and initial transient force response depend on K_{max} and strain, for both slow-pulling and fast pulling cases. Initial transient force is a stronger function of strain when the cell is experiencing rapid pulling. (B) Initial transient force is a function of strain rate.

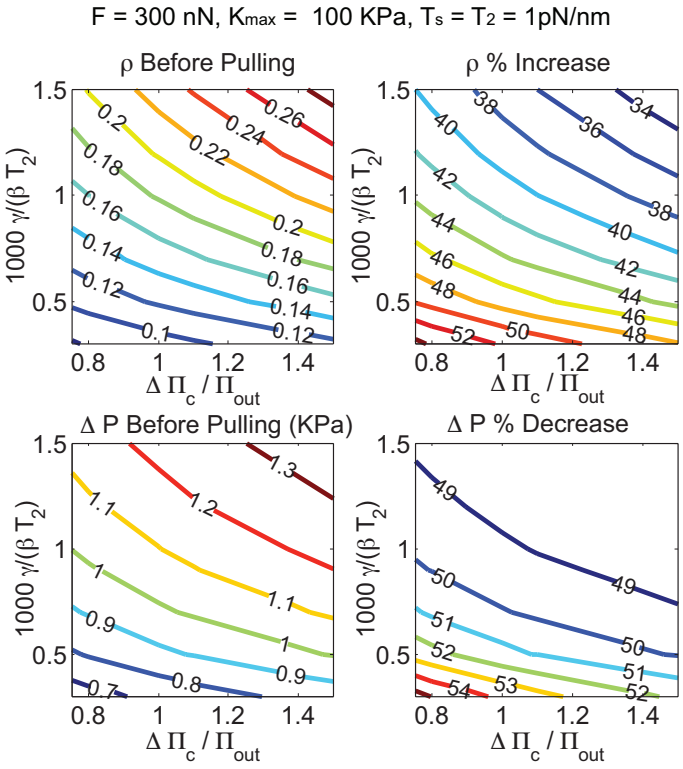

FIG. 5. Ion flux effects when a cylindrical cell is subjected to a mechanical force jump of 300 nN (Fig. 6 in the main text). Rho activation and pressure increases with higher ion inflow, but the unrecovered ratios of Rho and pressure differences also become larger.

to changes in μ [3], and therefore affect myosin force production. For the same deformation rate, a strongly cross linked actin network will result in higher myosin force if our model is correct. However, although our model successfully predict the strain-rate dependence of cell tension under mechanical strain, the unrecovered force is larger than it is observed in the experiment. Moreover, in the experiment, the force response during fast, "step-function"-like pulling is actually lower than the fast-pulling case. This is because in our model, we assume prefect cylindrical cell shape throughout the pulling process, which is not true in the real cell. When the cell is initially pulled, volume change is not instantaneous and dr/dz is not equals to zero. Nevertheless, if we neglect complex short time mechanics, the simple model predicts long term cell tension response and displays essential elements of force-recovery and strain-rate response.

ADDITIONAL RESULTS ON CYLINDRICAL CELL UNDER MECHANICAL PULLING FORCE

In Fig. 4, we show that for a small vertical deformation, both long term steady state force and short term initial force response depend on myosin contraction and strain rate. In the experimental studies, it was shown that the time-dependent force curve is almost smooth for pulling rate of 10 micrometer per minute, while a small jump is observed when pulling rate is 1 μm per min. The jump is even higher when a step-function-like displacement is applied. This is qualitatively reproduced in our model. Furthermore, the model shows that such force jumps depend on K_{max}, a parameter that is a function of total available myosin. Here we use $K_{max} = 50$ to 60 KPa to match the experimental results.

In the main text, we showed the cell volume, membrane tension and Rho activation level are able to recover when cell is subject to a small tensile force. This is due to the active response of myosin contraction, as well as osmotic

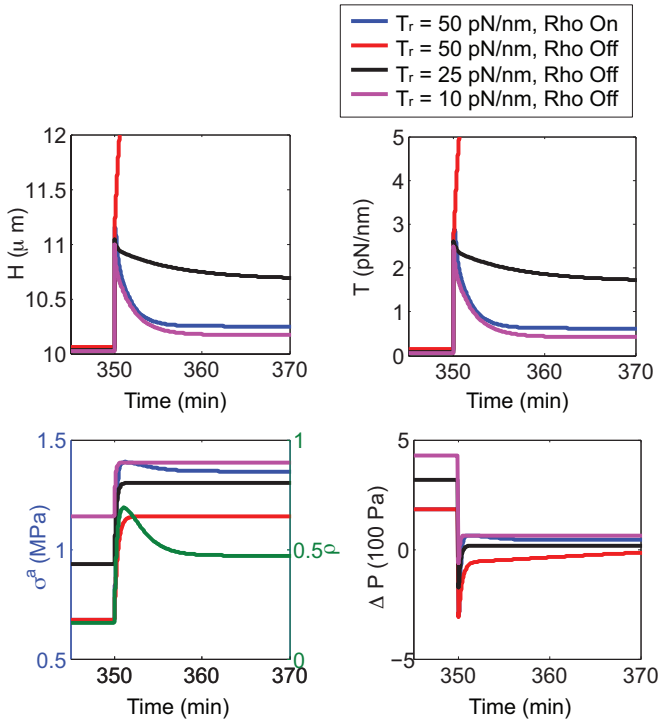

FIG. 6. Comparisons between models with and without Rho signaling and shear dependent myosin activity for cells with a force jump of 300nN at $t = 0$. T_r is the parameter describing the level of shear stress dependence in myosin activity. If Rho signaling is turned off, T_r has to decrease by a factor of 5 in order to obtain similar recovery dynamics.

content adjustment. Here, we will discuss how ion fluxes affect the cell recovery process.

Again, we use dimensionless parameters $\frac{1000\gamma}{\beta T_2}$ and $\frac{\Delta\Pi_c}{\Pi_{out}}$ to describe the overall ion content changes inside the cell before and after pulling. Fig. 5 shows results when a 300 nN pulling force is applied at $z = H$. Both $\frac{1000\gamma}{\beta T_2}$ and $\frac{\Delta\Pi_c}{\Pi_{out}}$ affect the steady state pressure and Rho activation. Ion fluxes become larger when we increase these parameters. Increasing ion fluxes increases the steady state pressure and decreases the permanent pressure change after pulling. However, increasing pressure also results in higher membrane and cortical tension, and thus activated Rho also can change significantly. In the main text, we chose parameters such that ΔP is below 1kPa.

Since this model involves several parallel mechanisms that controls cellular force response, it would be interesting to investigate the situation when one of the mechanisms is disabled. For example, we want to see whether the cell can still respond to external mechanical force if the Rho signal network has been disabled. The hypothetical simulation result for the force response is shown in Fig. 6. Under the same myosin assembly parameter (same T_r), turning off Rho network disables cell tension recovery, unless a_2 is a stronger function of T_{shear}. Physically speaking, myosin assembly and contraction have to be more sensitive to transient stress in order for tension recovery if Rho signal network is disabled. This suggests that the cell tension response system is more robust if both mechanisms are involved. However, this also suggest that cytoskeletal structures alone may be able to maintain cell volume and tension without Rho activation in some situations. These redundant mechanisms may explain robustness of cell shape and mechanics in varying environments.

[1] Tinevez, J.Y., U. Schulze, G. Salbreux, J. Roensch, J. F. Joanny, and E. Paluch. 2009. Role of cortical tension in bleb growth. PNAS. 106: 18581-18586.

[2] Petrie, R.J., H. Koo, and K. M. Yamada. 2014. Generation of compartmentalized pressure by a nuclear piston governs cell motility in a 3D matrix. Science, 345:1062-1065.

[3] Wirtz, D. 2009. Particle-Tracking Microrheology of Living Cells: Principles and Applications. Ann. Rev. Biophys. 38:301-326.

[4] Danuser, G. and C. M. Waterman-Storer. 2006. Quantitative fluorescent speckle microscopy of cytoskeleton dynamics. Annu. Rev. Biophys. Biomol. Struct. 35:361-387.

[5] Amano, M., K. Chihara, K. Kimura, Y. Fukata, N. Nakamura, Y. Matsuura, and K. Kaibuchi. 1997. Formation of Actin Stress Fibers and Focal Adhesions Enhanced by Rho-Kinase. Science 275:1308-1311.

[6] Webster, K. D., W. P. Ng, and D. A. Fletcher. 2014. Tensional homeostasis in single fibroblasts. Biophys. J. 107: 146-155.

[7] Luo, T., K. Mohan, P. A. Iglesias, and D. N. Robinson. 2013. Molecular mechanisms of cellular mechanosensing. Nat. Mater. 12: 1064-1071.

[8] Veigel, C., J. E. Molloy, S. Schmitz. and K. Kendrick-Jones. 2003. Load dependent kinetics of force production by smooth muscle myosin measured with optical tweezers. Nat. Cell Biol., 5:980-986.

TABLE I. Parameters in the model. These parameters are obtained from estimates of typical eukaryotic tissue cells. The rate parameters (a_1, a_2, d_1, d_2) are unknown and adjusted to match experiments.

Parameter	Value	Description
a_1	5/min	Activation rate of Rho
a_2	5/min	Activation rate of MLC
d_1	5/min	Deactivation rate of Rho
d_2	5/min	Deactivation rate of MLC
A_0	$(4 \sim 10) \times 10^3 \mu\text{m}^2$	Reference (unstretched) cell membrane area
T_c	0 pN/nm	Critical tension for Rho activation
T_s	0.8∼2 pN/nm	Saturation tension for Rho activation
T_1	0 pN/nm	Critical tension for MS ion channel opening
T_2	0.8∼2 pN/nm	Saturation tension for MS ion channel
Π_{out}	0.3∼ 0.5 MPa	Osmotic pressure in the extracellular environment
$\frac{\Delta\Pi_c}{\Pi_{out}}$	$0.1 \sim 2$	Critical osmotic pressure for ion pump
h	0.5μm	Cortical layer thickness
K_{max}	$10 \sim 500$ KPa	Maximum active contractile stress
κ	20 pN/nm	Effective elastic modulus of the membrane
α	30,000 nm^3 /(pN s)	Permeation constant for water flux
β	10^{-23} mol nm/(pN^2 s)	Permeation constant for MS ion channel
γ	0.05 ∼1.5 X $10^{-3}\beta T_2$mol/(s pN)	Permeation constant for ion pump flux